# Conformations and Rotational Barriers of (*Z*)-1,2-α-Naphthostilbene Crown Ethers and Their Alkali Metal Complexes

**Andreas Merz*, Lutz Gromann, Andreas Karl, T. Burgemeister, and F. Kastner**

Institut für Organische Chemie der Universität Regensburg,
D-93040 Regensburg, Germany

Received May 17, 1996

**Key Words:** Calculations, force field / Dynamic NMR spectroscopy / Chiral conformations / Chiral ion pairs

The synthesis of 2,3-didehydro[15]crown-5 and -[18]crown-6 derivatives **4a**, **b** with vicinal α-naphthyl groups at the double bonds starting from α-naphthoin (**3**) is described. The barriers to rotation of the naphthyl groups were probed by MM2 and by dynamic $^1$H-NMR spectroscopy. An achiral *syn* and a chiral *anti* conformation were experimentally observed at −90 °C for the free ligands and at −40 °C for the complexes. The experimental $\Delta G^{\neq}$ and the calculated $\Delta H^{\neq}$ values are in fair agreement. The barriers are substantially higher in the alkali metal complexes than in the free ligands. In the presence of racemic and potassium *S*-(+)-mandelate non-equilibrating ion pairs with **4b** were observed by low-temperature $^1$H-NMR spectroscopy for the *anti* conformation.

Naphthyl groups frequently show hindered rotation in a sterically crowded environment, especially when the aromatic ring is linked by the α-position. Anderson and coworkers provided an example by dynamic $^1$H-NMR studies and MM2 calculations on 1-vinyl-naphthalenes with increasing methyl substitution in the remaining vinylic positions[1]. Whereas one single methyl group in any of the olefinic positions is not sufficient to create a rotational barrier detectable by low-temperature NMR spectroscopy, the trimethyl compound has a rotational barrier of 14.3 kcal/mol at 263 K. A related example is the rotation of an α-naphthyl group in a tertiary amine[2].

In the course of our studies of unsaturated crown ethers[3a–d] we prepared the α-naphthostilbene [15]crown-5 and [18]crown-6 ethers **4a** and **4b** which likewise show a restricted rotation of the two vicinal naphthyl groups. In this work we report on the roational barriers as a function of the size of the crown ethers, both as free ligands and the complexes **1a** · NaSCN and **1b** · KSCN. Experimental data were obtained by dynamic $^1$H NMR spectroscopy for all species. MM2 calculations on the free ligands **4a** and **4b** are in fair agreement with the experimental findings.

## Syntheses

**4a** and **4b** were prepared from α-naphthoin (**3**)[3a]. Since the classical benzoin condensation of 1-naphthaldehyde (**1**) gave only a very poor yield of **3**[4], we used a protocol of Hünig et al.[5] as given Scheme 1. Aldehyde **1** was converted into the *O*-(trimethylsilyl)cyanohydrin **2a**, the carbanion **2b** of which was added to the parent aldehyde to give 1,1-naphthoin (**3**) in 53% overall yield. The direct ring closure between **3** and the suitable oligoethylene glycol dimesylate affording **4a** or **4b** was achieved with powdered KOH in dry THF. The use of the mesylate leaving group under these conditions proved to be the best choice in many crown ether syntheses in our laboratory[3c]. Both crown ethers are formed in good yield as crystalline compounds.

Scheme 1

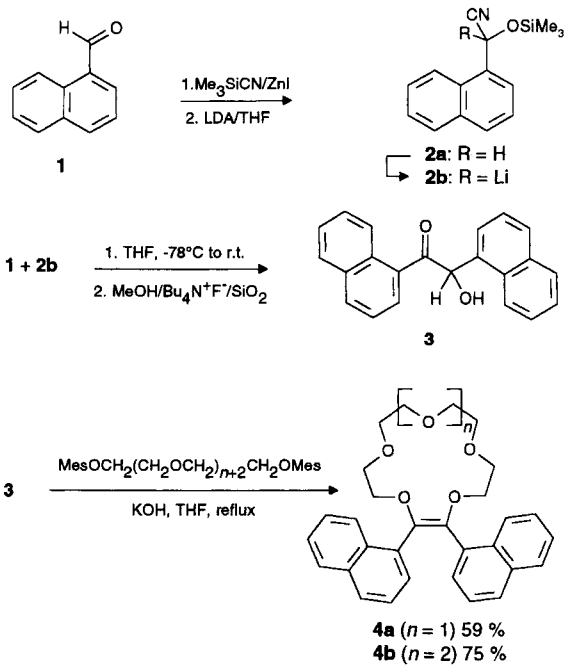


## MM2 Calculations

The structures with *syn* or *anti* orientation of the α-naphthyl substituents shown in Scheme 2 are obviously main conformations of **4a** and **4b** which are interconverted by rotation of one of the naphthyl rings around its bond to the adjacent sp$^2$ carbon.

  0947–3440/96/1010–1635 $ 15.00+.25/0 

Scheme 2

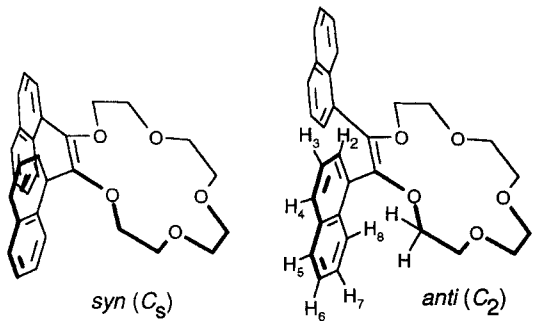


The steric hindrance is expected to occur when 2-H and 3-H are passed alongside the second naphthyl ring and 8-H simultaneously moves past the adjacent $CH_2$ group of the crown ether. Ideally, the *syn* conformation is a $C_s$ symmetric *meso* form whereas the chiral *anti* conformation has $C_2$ symmetry.

The *syn* and *anti* structures were geometry-optimized for **4a** and **4b** by using the MM2 force field[6], and their heats of formation were calculated. For the determination of the transition states by MM2 beginning with the *syn* conformation, one naphthyl ring was rotated and the second one was allowed to yield synchronously, thus following a minimized energy gradient until the maximum was reached with one of the naphthyl rings almost coplanar to the double bond. The stick models of the *syn* and *anti* conformations and the transition-state structure of **4b** according to MM2 are shown in Figure 1. Neither the *syn* nor the *anti* structure show the idealized symmetries given in Scheme 2 because one of the dioxyethylene groups adjacent to the double bond exhibits a *gauche*, the other an *anti* conformation. This is a typical structural detail known from crystal structures of unsaturated or benzofused crown ethers[3c,7]. However, the local symmetry of the naphthostilbene unit was confirmed for each conformer. In the *syn* conformation the planes of the naphthyl groups are twisted by an angle of 64° out of the plane of the double bond, in the *anti* conformation this angle is 113° (based on the starting conformation). Obviously, in these conformations there is a favorable balance of π conjugation, aromatic π stacking and avoidance of steric hindrance with the adjacent $CH_2$ group. The position of naphthyl groups in the transition state is similar to that in the crystal of the parent hydrocarbon (*Z*)-naphthostilbene[8] where there is no steric hindrance from opposite substituents.

On the way from the transition state down to the *anti* conformation the MM2 calculation finds a shallow hump for both **4a** and **4b** in the energy curve representing a "pre-*anti*" form with an angle of 72°. The energy of these metastable conformations is only ca. 0.8 kcal higher than the final ones. The transformation of the transition state into the pre-*anti* form is accompanied by a conformational reorientation of the crown ether ring: the *gauche* and *anti* ethylenedioxy groups at the double bond are interchanged. The entire process is documented in the structures depicted in Figure 1.

The calculated heats of formation of the conformers and the transition states for **4a** and **4b** are given in Table 1. The *anti* forms represent the absolute minima for both crown ethers but the *syn* conformation of **4b** is only 0.2 kcal/mol higher in energy, and for **4a** this difference is negligible. The energy barriers between *syn* and *anti* are in the range of 13 kcal/mol and suggest that the observation of the conformations by low-temperature NMR spectroscopy should be possible. MM2 calculations could not be performed on the alkali metal complexes due to lack of suitable parametrization for the cation-to-oxygen bonds. However, we reasoned that th $CH_2$ groups adjacent to the naphthostilbene

Figure 1. MM2-optimized geometries for the *syn* and *anti* conformations of **4b** and the transition state

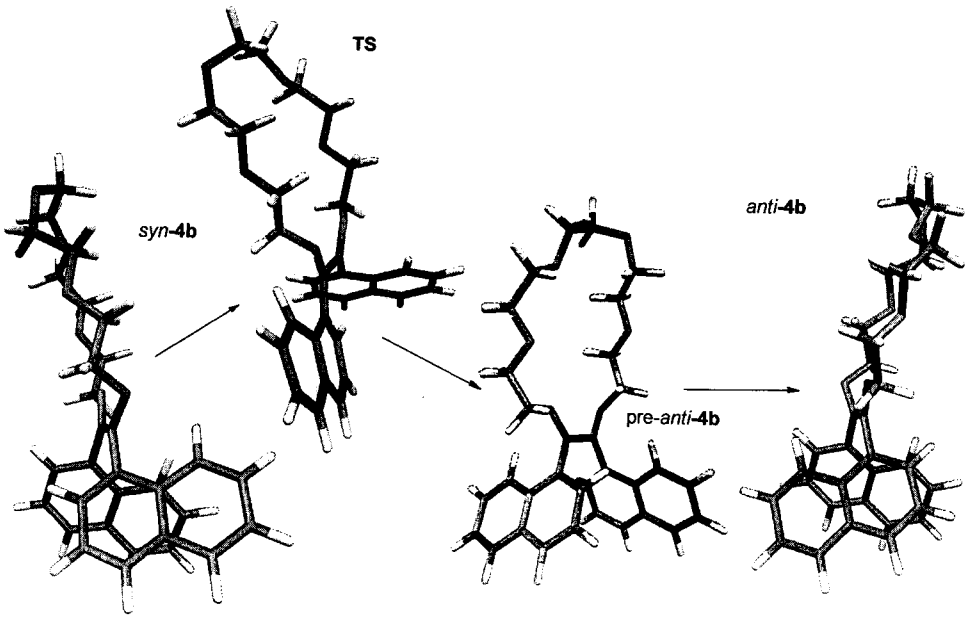

group would be forced outward by the complexed cation and would thus represent a stronger obstacle to the rotation of a naphthyl group.

Table 1. Calculated MM2 activation enthalpies of **4a** and **4b** and experimentally determined free energies of activation for **4a** and **4b** and their complexes for the conformational equilibria

| Compounds | MM2 data [kcal] | | | | | | $^1$H-NMR data | |
|---|---|---|---|---|---|---|---|---|
| | $\Delta H_f(syn)$ | $\Delta H_f(anti)$ | $\Delta\Delta H_f$ | $\Delta H_f$(TS) | $\Delta H^{\neq}$ | $\Delta\Delta G$ | $T_c \pm$ 10 [K] | $\Delta G^{\neq}(T_c)$ ± 0.5 |
| **4a** | −80.36 | −80.39 | 0.03 | −68.00 | 12.38 | 0.43 | 248 | 11.4 |
| **4a** • NaSCN | — | — | — | — | — | 0.43 | 273 | 13.4 |
| **4b** | −121.71 | −121.88 | 0.17 | −108.90 | 12.90 | 0.64 | 253 | 12.0 |
| **4b** • KSCN | — | — | — | — | — | 0.64 | 297 | 14.6 |

## Dynamic $^1$H-NMR Spectroscopy

The room-temperature 400-MHz $^1$H-NMR spectrum of **4b** is shown in Figure 2 (top). Indeed, even at 294 K a beginning broadening of the 2-H signal is visible. The assignments of all naphthalene protons in this spectrum was confirmed by a COSY spectrum. For **4a** the first sign of broadening is found at 183 K. At 273 K, the whole ensemble of the protons 2-, 3-, 6-, and 7-H is involved in further broadening, and at 253 K only proton 4-H still gives rise to a sharp doublet. This signal remains unchanged over the entire temperature range. At 233 K a sharp set of naphthalene protons reappear while there are still smaller broadened signals. The complete separation of the spectrum into the two final naphthalene spectra is reached at 193 K. The integration of the two low-field doublets corresponding to the 8-H protons gives a ratio of ca. 6:1 for **4b** (shown in Figure 2, bottom left) and 3:1 for **4a**. The assignment of the major conformer to the *anti* conformation is based on the upfield chemical shifts of 2-H and 3-H on both naphthyl rings which, vice versa, reach the shielding cone of the adjacent naphthyl ring (see also Scheme 2). In the minor conformer these protons suffer a significant *downfield* shift from the outer ring current of the neighboring ring as expected for the *syn* conformer. The chemical shift data are given in Table 2.

As expected from the above discussion the changes in the NMR spectra of the complexes should occur at substantially higher temperatures. This is clearly the case: **4a** · NaSCN and **4b** · KSCN exhibit broadened $^1$H-NMR spectra at room temperature, resembling the 253-K spectra of the free ligands. In order to obtain averaged spectra the probes have to be heated at ≥400 K in $C_2D_2Cl_4$ (250 MHz). The clean separation of *syn* and *anti* conformers is already

Figure 2. Variable-temperature $^1$H-NMR spectra of **4b** and **4b** · KSCN in $CD_2Cl_2$; only the naphthalene protons are shown, for chemical shift data see Table 2 and Experimental

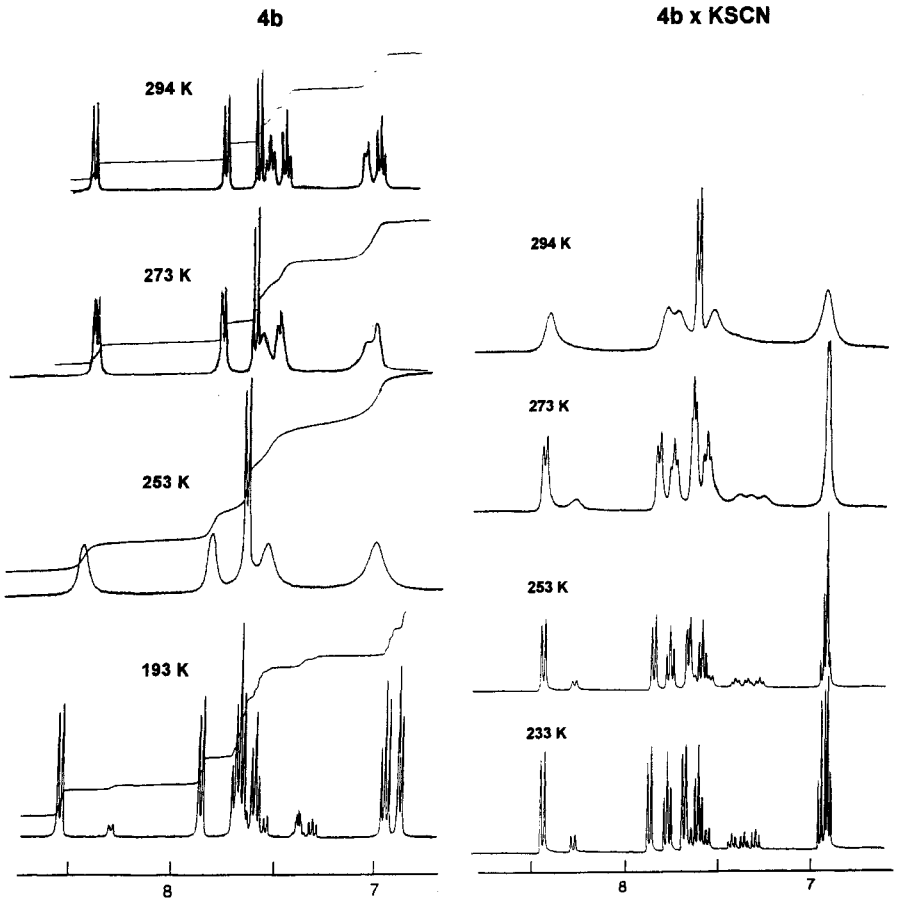

Table 2. $^1$H-NMR chemical shifts δ of the naphthalene protons for the averaged spectra and the *syn* and *anti* conformations of **4a** and **4b** and their complexes

| | | 2-H | 3-H | 4-H | 5-H | 6-H | 7-H | 8-H |
|---|---|---|---|---|---|---|---|---|
| **4a** | average | 7.04 (d) | 6.95 (t) | 7.56 (d) | 7.73 (dd) | 7.43 (dt) | 7.48 (dt) | 8.41 (dt) |
| | *syn* | [a] | [a] | [a] | [a] | [a] | [a] | 8.30 |
| | *anti* | 6.97 | [a] | [a] | 7.86 | [a] | [a] | 8.52 |
| **4a** • NaSCN[b] | | 7.17 | 7.02 | 7.57 | 7.67 | 7.41 | 7.59 | 8.32 |
| | *syn* | [a] | [a] | [a] | [a] | | 7.3-7.4 | 8.33 |
| | *anti* | 7.01 | 7.03 | 7.69 | 7.86 | 7.59 | 7.99 | 8.48 |
| **4b** | average | 7.02 (d) | 6.94 (t) | 7.55 (d) | 7.73 (dd) | 7.43 (dt) | 7.48 (dt) | 8.38 (dt) |
| | *syn* | 7.52 (d) | 7.30 (t) | [a] | [a] | 7.36 (t) | 7.38 (t) | 8.30 (d) |
| | *anti* | 6.86 (d) | 6.93 (t) | 7.65 (d) | 7.86 (d) | 7.58 (t) | 7.68 (t) | 8.56 (d) |
| **4b** • KSCN[c] | | 7.09 | 6.95 | 7.65 | 7.51 | 7.38 | 7.54 | 8.28 |
| | *syn* | 7.45 | 7.31 | [a] | [a] | 7.38 | 7.44 | 8.26 |
| | *anti* | 6.87 | 6.95 | 7.69 | 7.88 | 7.62 | 7.78 | 8.42 |

[a] Signals not discernible. – [b] In $C_2D_2Cl_2$ at 138 °C. – [c] In $C_2D_2Cl_2$ at 120 °C.

complete at 253 K (400 MHz) as shown in Figure 2 (right side). Thus, the process is slower in the complexes but the ratio of the conformers is the same in the free ligand and the complex. Apart from slight temperature-induced shifts no changes in the spectra are observed any more down to 193 K.

### Comparison of MM2 and NMR Data

The determination of a definite coalescence temperature $T_c$ for this conformational equilibrium is difficult, because the line broadening is a multiple-proton process, and the ratio of conformers is not unity. The larger signals get reshaped earlier than the small ones. The analysis of this process by the simple equation for a symmetric first-order one-signal case, which is uded here, can only be a rough estimation under these circumstances. The state of maximal broadening is taken as the "coalescence temperature" with an estimated accuracy of −10 K. The data thus obtained are given in Table 1 together with the MM2 data of the free ligands.

Overall, the calculated and experimental data are in fair agreement considering the uncertainties in the comparison of $\Delta H^{\neq}$ and $\Delta G^{\neq}$ values. In particular, the differences in the crown ether sizes are found by both methods. Apparently, the smaller crown ether causes less sterical hindrance at the $=CH-OCH_2-$ position. The free energy difference of the two conformers calculated from the ratio is 0.64 kcal/mol for **4b** and 0.43 kcal for **4a**, the $\Delta H_f$ values obtained by MM2 are smaller but follow the same direction.

Remarkably, the difference in conformational mobility of the free ligand and the complex is significantly higher for **4b**. This finding suggests that the structures of the free ligand and the corresponding complex are more similar to each other in the [15]crown-5 derivatives than in the case of [18]crown-6 systems. In the complexes, all ethylenedioxy units are in a more or less *gauche* orientation[7a]. Thus, the $CH_2$ groups adjacent to the naphthostilbene group are forced outward. Free [18]crown-6 derivatives form a compact conformation with two *anti* $-O-CH_2CH_2-O$ groups connected by pairs of *gauche* ones[7a]. In unsaturated crown ethers one of each type *must* be connected to the double bond[3c,7]. In [15]crown-5-systems this geometry is not possible, and the free ligands have indeed less compact structures than their 18-membered homologues[9].

### Ion-Pair Formation at Low Temperature

Although the assignment of the *syn* and *anti* conformation in the NMR spectra is clear from chemical shift interpretation, we have attempted to verify the chirality of the *anti* cornformation by interaction with mandelate salts as hosts and simultaneous chiral shift reagents[10]. For this purpose, the complexes of **4b** with potassium (*S*)-(+)-mandelate and the racemic salt were studied by variable-temperature $^1$H-NMR in $CD_2Cl_2$. We anticipated rapidly equilibrating ion pairs on the NMR time scale at low temperature. Thus, in the racemic case, the NMR spectra should be similar to those of the KSCN salt (Figure 2). In the chiral case, one or more signals of the *anti* form should split into pairs of equal intensity[10]. The proton 8-H is taken as an indicator.

Figure 3. Variable-temperature $^1$H-NMR signals of the 8-H naphthalene protons of complexes of **4b** with the potassium salts of racemic and (*S*)-(+)-mandelic acid

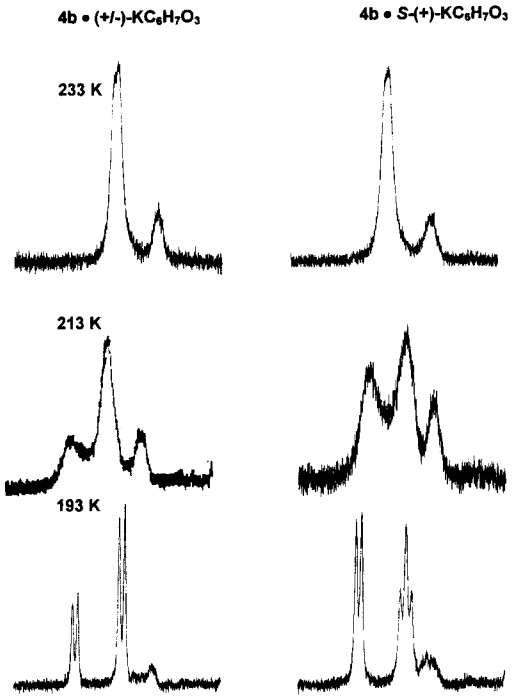


Down to 233 K both probes show the same behavior as the KSCN salt, but the signals do not become sharper (Figure 3). Instead, a new dynamic process is apparent at 213 K. Finally, at 193 K the *anti*-8-H signals of *both* probes appear as two signals at δ = 8.56 and 8.38 with an intensity ratio of 2:3. This finding points to the formation of ion pairs which do no longer interconvert on the NMR time scale. Thus, whith the racemic mandelate salt the racemates of diastereomeric ion pairs are formed while in the optically active case pure enantiomers of these ion pairs are present.

The chemical shifts are the same in both cases. As a further detail, the upfield doublet of the *anti* form shows a further splitting into two doublets of *equal* intensity. This could be attributed to a higher association form of the ion pairs which must be an equilibrium effect since it is not found in the racemic environment. All other naphthalene signals of the crown ether and mandelate proton signals are sharp and unchanged below 233 K.

The 8-H signal of the *syn* conformation remains broadened even at 193 K. Ion pairs of this conformation could, in principle, show split signals for the protons 8-H of non-equal intensity due to the non-homotopic faces because the $C_s$ symmetry is broken by the chiral anion. The whole process is much more complex than the equilibrium case[10]. As expected, the detailed NMR results depend on the concentration and on the ratio of the crown ether to the mandelate salt.

This work was supported by the *Fonds der Chemischen Industrie.*

## Experimental

IR: Beckman Acculab 1 or 2. – UV/Vis: Hitachi U 2000. – $^1$H and $^{13}$C NMR: Bruker AW 80, Bruker WM 250 or Bruker ARX 400, TMS as internal standard in $CDCl_3$ unless noted otherwise). – EI-MS (70 eV): Varian MAT 112 S. – Melting points (uncorrected): Büchi 510 apparatus. – Elemental analyses: Analytical Laboratory of the University of Regensburg.

*1-[Cyano(trimethylsiloxy)methyl]naphthalene* (**2a**): Preparation adapted from ref.[5]. A mixture of 1-formylnaphthalene (**1**) (3.12 g, 20 mmol), cyanotrimethylsilane (2.18 g, 2.70 ml, 22 mmol), and dry $ZnI_2$ (50 mg) is heated at 100°C for ca. 8 h (IR control for C=O). The product is distilled in a kugelrohr (120°C/0.02 bar) to give **2a**; 4.85 g (19 mmol, 95%), colorless crystals, m.p. 34°C. – IR (KBr): $\tilde{\nu}$ = 3060 cm$^{-1}$, 2960, 2900, 1600, 1260, 1100, 1070. – $^1$H NMR (250 MHz): δ = 0.24 (s, 9H, $SiMe_3$), 6.09 (s, 1H, C*H*OH), 7.47–7.75 (m, 5H, naphthyl 2,3,4,6,7-H), 7.92 (d, 1H, naphthyl 5-H), 8.22 (d, 1H, naphthyl 8-H). – $C_{15}H_{17}NOSi$ (255.4): calcd C 70.54, H 6.70, N 5.48; found C 70.57, H 6.71, N 5.48.

*2-Hydroxy-1,2-di-1-naphthylethanone* (1,1′-Naphthoin, **3**): To an LDA solution prepared from diisopropylamine (1.72 g, 2.40 ml, 17 mmol) in DME (20 ml) and 1.6 M *n*-butyllithium in hexane (11.25 ml, 18 mmol) at –78°C, a solution of cyanohydrin **2a** (2.62 g, 17 mmol) in DME (4 ml) is added dropwise, and the mixture is stirred at –78°C for 30 min to give anion **2b**. Then a solution of **1** (2.65 g, 17 mmol) in DME (4 ml) is added, and the mixture is stirred for another 30 min. The entire following work-up procedure must be performed under nitrogen in order to prevent excessive oxidation to naphthil. After warming up to room temp., saturated aqueous $NaHCO_3$ (50 ml) is added to reaction mixture, and the product is extracted with diethyl ether (4 × 20 ml). Evaporation of the solvents from the combined extracts affords a yellow oil (6.20 g) which is dissolved in EtOH/THF (7.5 ml each), and the solution is stirred with tetrabutylammonium fluoride on $SiO_2$ (Fluka, 100 mg) for 24 h at room temp. The filtered solution is concentrated to give a yellow solid which is recrystallized from diethyl ether to give pure colorless crystals of **3**, 2.46 g (7.9 mmol, 53%), m.p. 137–138°C (ref.[11] 138–139). – IR (KBr): $\tilde{\nu}$ = 3460 cm$^{-1}$, 3040, 2960, 1665, 1585, 1565. – $^1$H NMR (250 MHz): δ = 4.74 (br. s, 1H, OH), 6.69 (s, 1H, C*H*OH), 7.17–7.83 (m, 12H, 2,3,4,5,6,7-H, both naphthyl rings), 8.29 (d, 1H, 8-H, CHOH naphthyl), 8.70 (d, 1H, 8-H, CO-naphthyl). – EI-MS, *m/z* (%): 312 (4) [M$^+$], 157 (29), 155 (100), 127 (43).

*2,3-Didehydro-2,3-di-1-naphthyl[15]crown-5* (**4a**) *and 2,3-Didehydro-2,3-di-1-naphthyl[18]crown-6* (**4b**): A mixture of naphthoin (**3**) (0.1 M in THF), an equimolar amount of tetra- or pentaethylene glycol dimesylate and powdered KOH (10-fold molar excess) is stirred at reflux temp. for 24 h. Initially, a deep orange-red color is observed due to the formation of the dianion of **3**. The filtered THF solution is combined with $CH_2Cl_2$ and water (3-fold volume each) and neutralized wih a few drops of 2 N HCl. The organic phase is washed with water (4 × 30 ml), dried ($MgSO_4$), and concentrated. The remaining oil is taken up in a minimum amount of diethyl ether, and the resulting solution is adsorbed on silica gel in a short column (1.5 × 15 cm). 50 ml of diethyl ether is passed through the column, and the eluate is discarded. The loaded silica is continuously extracted with diethyl ether for 12 h in a small Soxhlet apparatus. From the extract a colorless solid is isolated which is recrystallized from ethyl acetate.

**4a** [from 1.45 g (4.6 mmol) of **3**]: Yield 1.29 g (2.27 mmol, 59%), colorless crystals, m.p. 148–150°C. – UV ($CH_3CN$): $\lambda_{max}$ (ε) = 216 (10820). – IR: $\tilde{\nu}$ = 3040 cm$^{-1}$, 2920, 2870, 1640, 1590, 1450, 1150, 1090. – $^1$H NMR (250 MHz): δ = 3.72–3.88 [m, 16H, $O(C_2H_4O)_4$], naphthalene H, assignments by COSY: 6.95 (t, 2H, 3-H), 7.04 (d, 2H, 2-H), 7.43 (dt, 2H, 6-H), 7.48 (dt, 2H, 7-H), 7.56 (d, 2H, 4-H), 7.73 (dd, 2H, 5-H), 8.41 (dd, 2H, 8-H), coupling constants [Hz] in the naphthalene systems of **4a** and **4b**: $^2J_{2,3}$ = 6.8, $^4J_{2,4}$ = 1.23, $^2J_{3,4}$ = 7.8, $^2J_{5,6}$ = 8.0, $^4J_{5,7}$ = 1.6, $^2J_{6,7}$ = 6.4, $^4J_{6,8}$ = 1.2, $^2J_{7,8}$ = 8.4. – EI-MS, *m/z* (%): 470 (29) [M$^+$], 155 (100) [$C_{10}H_7CO^+$], 127 [$C_{10}H_7^+$], 45 (44) [$C_2H_4O^+$]. – $C_{30}H_{30}O_5$ (470.6): calcd. C 76.57, H 6.42; found C 76.44, H 6.40.

**4b** [from 1.16 g (3.7 mmol) of **1**]: Yield 1.43 (2.8 mmol, 75%) colorless needles, m.p. 93–94°C. – UV ($CH_3CN$): $\lambda_{max}$ (ε) = 216 (11670). – IR (KBr): $\tilde{\nu}$ = 3040 cm$^{-1}$, 2920, 2870, 1640, 1590, 1450. – $^1$H NMR (250 MHz): δ = 3.72–3.88 [m, 16H, $O(C_2H_4O)_4$], naphthalene H assignments by COSY: 6.94 (t, 2H, 3-H), 7.02 (d, 2H, 2-H), 7.43 (dt, 2H, 6-H), 7.48 (dt, 2H, 7-H), 7.55 (d, 2H, 4-H), 7.73 (dd, 2H, 5-H), 8.38 (dd, 2H, 8-H), coupling constants like in **4a**. – FD-MS ($CH_2Cl_2$): 514 [(M + 1)$^+$], 515 [M$^+$]. – $C_{32}H_{34}O_6$ (514.6): calcd. C 74.68, H 6.66; found C 74.51, H 6.60.

*Alkali Metal Thiocyanate and Mandelate Complexes of Crown Ethers* **4a** *and* **4b**: A solution of the ligand in $CH_2Cl_2$ is stirred for 24 h with an excess of the finely powdered alkali salt. The filtered solution is concentrated, and some drops of pentane is added to precipitate the crystalline complex.

**4a · NaSCN**: 69% yield, colorless crystals, m.p. 250°C (dec., ethyl acetate). – IR (KBr): $\tilde{\nu}$ = 3050 cm$^{-1}$, 2920, 2060, 1680, 1580, 1450, 1110. – $^1$H NMR (250 MHz): see Table 2. – $C_{30}H_{30}O_5$ · NaSCN: calcd. C 67.49, H 5.48, N 2.54; found C 67.25, H 5.51, N 2.48.

**4b · KSCN**: 75% yield, colorless crystals, m.p. 215–216 (ethyl acetate). – IR (KBr): $\tilde{\nu}$ = 2920 cm$^{-1}$, 2880, 2060, 1630, 1450, 1100. – $^1$H NMR see Table 2. – $C_{32}H_{34}O_6$ · KSCN: calcd. C 62.84, H 5.60, N 2.29; found C 62.17, H 5.67, N 2.36.

**4b · $C_8H_7KO_3$**: 78% yield from **4b** and *rac*-potassium mandelate, colorless crystals, m.p. 74–78°C.

**4b · (S)-$C_8H_7KO_3$**: 89% from **4b** and potassium (*S*)-(+)-mandelate, colorless crystals, m.p. 84–88°C.

[1] J. E. Anderson, D. J. Barkel, J. E. Parkin, *J. Chem. Soc., Perkin Trans. 2*, **1987**, 955–959.
[2] D. Casarini, L. Lunazzi, D. Macciantelli, *Tetrahedron Lett.* **1984**, K 3641–3642.
[3] [3a] A. Merz, *Angew. Chem.* **1977**, *89*, 484–485; *Angew. Chem. Int. Ed. Engl.* **1977**, *16*, 467–468. – [3b] A. Merz, F. Dietl, R. Tomahogh, G. Weber, G. M. Sheldrick, *Tetrahedron* **1984**, *40*, 665–671. – [3c] A. Merz, A. Karl, T. Futterer, N. Stacherdinger,

O. Schneider, J. Lex, E. Luboch, F. Biernat, *Liebigs Ann. Chem.* **1994**, 1199–1209.
[4] M. Gomberg, F. J. van Natta, *J. Am. Chem. Soc.* **1929**, *51*, 2238–2245.
[5] K. Deuchert, U. Hertenstein, S. Hünig, G. Wehner, *Chem. Ber.* **1979**, *112*, 2045–2061; S. Hünig, G. Wehner, *ibid.* **1979**, *112*, 2062–2067.
[6] U. Burkert, N. L. Allinger, *Molecular Mechanics*, ACS Monograph No. 177, American Chemical Society, Washington, D. C., **1982**.
[7] [7a] R. Hilgenfeld, W. Saenger, *Top. Curr. Chem.* **1982**, *101*, 1–82; esp. pp. 38–40. – [7b] D. Bright, M. Truter, *J. Chem. Soc. (B)* **1970**, 1544–1550.
[8] S. M. Aldoshin, M. V. Alfimov, L. O. Atovmyan, V. F. Kaminsky, V. F. Razumov, A. G. Rachinsky, *Mol. Cryst. Liq. Cryst.* **1984**, *108*, 1–17.
[9] I. R. Hanson, *Acta Crystallogr., Sect B.*, **1978**, *34*, 1026–1028.
[10] W. H. Pirkle, D. J. Hoover, *Top. Stereochem.* **1982**, *13*, 263–331.
[11] H. Schubert, L. Selisko, *J. Prakt. Chem.* **1962**, *16*, 1–7.
[96128]